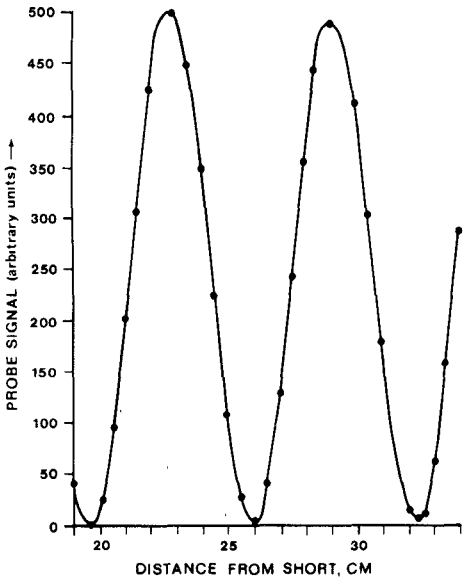

Fig. 6 Measurements with movable current probe on short-circuited coplanar waveguide. Probe signal (proportional to square of RF current) versus position $f = 1$ GHz

pearing in the waveguide because of the probe is

$$Z_W = \frac{v_W}{i_W} = \frac{\omega^2 M^2}{Z_L}. \tag{4}$$

If there were no spacing between the waveguide and the probe, M would be equal to Ll, where L is the waveguide's inductance per unit length and l is the width of the probe. To take account of the spacing s, we write $M = f(s)Ll$, where $f < 1$. Then making use of the property of TEM guide that $L = Z0k/\omega$ (where $k = 2\pi/\lambda_g$, and λ_g is the guide wavelength), we conclude that

$$Z_W = [(kl)f(s)Z_0]^2/Z_L. \tag{5}$$

If Z_W is purely resistive, the fraction of the line power extracted by the probe is approximately Z_W/Z_0.

Using device 2 in the probe of Fig. 5 at 1 GHz, with a spacing of 3 mm, the reflections seen on a network analyzer are less than 1 dB over the entire band 0.1–1.3 GHz. Line powers were measurable down to 3.5 μW, corresponding to a signal of 32 nV at the input of the lock-in amplifier. Using device 1, a much smaller line power, 23 nW would be measurable.

Standing-wave ratio and reflection coefficient can be measured by moving the current probe along the line, very much as one uses a conventional slotted line. Trial measurements were made in this way, using coplanar waveguide at 1 GHz. The probe was moved along a very simple plexiglass track, with no special effort at smoothness or precise alignment with the guide. A typical result, for the case of a shorted line, is shown in Fig. 6. This technique is especially useful for measuring low standing-wave ratios, which are difficult to measure by other means, because they are obscured by reflections at the feed point of the line. Because the bolometer is a square-law detector, small current variations are easily seen, and they can be distinguished from random alignment variations by their periodicity. SWR's as low as 1.02 have been observed.

At higher frequencies, it may be difficult to achieve smooth motion of the probe while maintaining a constant small spacing from the line. However, it seems feasible to fabricate several probes on a single substrate. Using a microscope, the array of probes would then be placed in a stationary position over the waveguide, with suitable spacers used to obtain the desired coupling. With an array density of 10 probes in a half-guide wavelength, it should be possible to determine reflection coefficient with fair accuracy. For the success of this method, it is necessary that the probes be nearly identical. However, the probes are not small, by photolithographic standards, and can be designed in such a way that mask alignment errors have little effect. Thus, the likelihood of achieving the necessary uniformity seems quite high.

ACKNOWLEDGMENT

The authors wish to thank Dr. J. G. Swansom for very useful discussions and assistance. Technical assistance was ably provided by B. Wood and T. Malik.

REFERENCES

[1] E. W. Strid and K. R. Gleason, "A dc-12 GHz monolithic GaAs FET distributed amplifier," *IEEE Trans. Microwave Theory Tech.*, vol. MTT-30, pp 969–75, July 1982.
[2] E. W Strid and K R. Gleason, "Calibration methods for microwave wafer probing," presented at 1984 Int. Microwave Symp., San Francisco, CA, May 30–June 1, 1984.
[3] T. Hwang, S. E. Schwarz, and D. B. Rutledge, "Microbolometers for infrared detection," *Appl Phys. Lett.*, vol. 34, pp. 773–76, June 1, 1979
[4] T Hwang, "Microbolometers for far-infrared detection," Ph.D. thesis, Univ. of California, Berkeley, 1979.
[5] D. P Neikirk and D B. Rutledge, "Air-bridge microbolometer for far-infrared detection," *Appl. Phys Lett.*, vol. 44, pp 153–55, 1984
[6] D. P Neikirk, W. W. Lam, and D. B. Rutledge, "Far-infrared microbolometer detectors," *Int. J. IR MM Waves*, vol. 5, pp. 245–78, Mar. 1984.
[7] D. P. Neikirk and D. B. Rutledge, "Far-infrared embedding impedance measurements," *Int. J. IR MM Waves*, vol. 5, pp. 1017–1026, July 1984.
[8] D. P. Neikirk, "Integrated detector arrays for high-resolution far-infrared imaging," Ph D. thesis, California Inst. of Technol., 1984.
[9] E W Washburn, Ed., *International Critical Tables*, 1st ed. New York: McGraw Hill, 1929, vo 4, pp. 105, 106, 229.

Analysis of Square-Spiral Inductors for Use in MMIC'S

PETER R. SHEPHERD

Abstract—**A method analysis of square spiral inductors for use in monolithic microwave integrated circuits (MMIC's) is presented. The method is based on the coupled microstrip-line theory and incorporates a novel solution to the multicoupled-line problem. The analysis includes the effect of the discontinuities at the right-angled bends in the lines, and also the feedback effect where the lead-out bridge crosses the lines. The method can be used to analyze components with an arbitrary number of spiral turns.**

Theoretical results are compared with the measured S-parameters of a $3\frac{1}{2}$-turn component over the range 2–12 GHz, and reasonable agreement between the two is found.

Manuscript received August 22, 1985; revised November 20, 1985. This work was supported in part by the Procurement Executive (DCVD), U. K. Ministry of Defense

The author is with the Microwave Solid-State Group, Department of Electrical and Electronic Engineering, University of Leeds, Leeds LS2 9JT, U.K.

IEEE Log Number 8407186

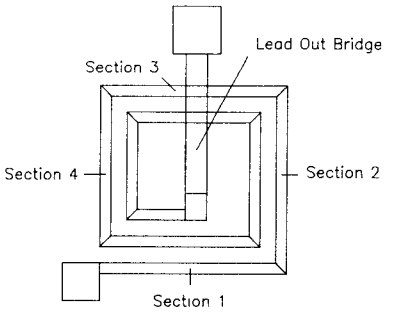

Fig. 1. Square spiral inductor.

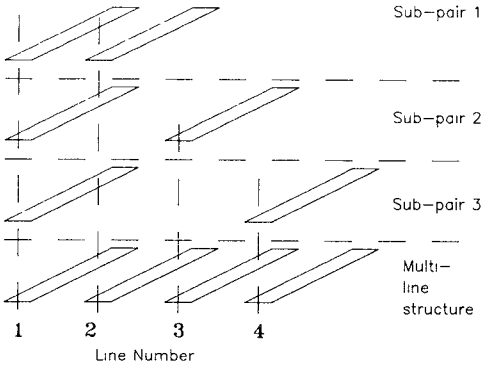

Fig. 2 Multitransmission line broken down into a series of two-coupled lines

I. Introduction

This paper is concerned with the analysis of square spiral inductor components as used in monolithic microwave integrated circuits (MMIC's). The layout of a typical component is shown in Fig. 1, and consists of a series of turns of thin metallized transmission lines laid on top of a dielectric (which may consist of layers of different dielectric material), and which usually has a metallized ground plane beneath the dielectric. The component also has some form of lead-out bridge which may either be under or over the spiral turns, and there may be a dielectric material, or air, between the bridge and the turns.

Past analyses of these components have included a calculation of the inductance of the transmission lines, taking into account the negative mutual inductance from coupling between two conductors having current vectors in opposite directions [1]. This analysis takes no account of the parasitics (capacitive coupling and loss) associated with the component structure. Recent analyses based on transmission-line theory [2], [3] have attempted to account for these effects, but these analyses are limited in the number of spiral turns with which they can cope. A method based on an electrostatic and magnetostatic analysis of the structure [4] appears to give reasonable results, but would be difficult to implement in a computer-aided design (CAD) package. The most common method of deriving equivalent circuits for these components is by measurement of a test component and use of an optimization algorithm to fit an equivalent circuit to the measured data, e.g., [5]. These methods rely on measurement data which may be of dubious quality. It is not a true theoretical analysis, and often the elements of the equivalent circuit cannot be related to the physical parasitics or effects of the component. It is more scientifically pleasing to be able to derive the characteristics of the element purely from its physical geometry and the known characteristics of the materials from which it is manufactured.

The object of this work is to derive the characteristics of these components (in the form of two-port S-parameters) which may have an arbitrary number of spiral turns, based on the coupled transmission-line theory, and taking into account the losses in the lines. The method, however, is in a simple enough form to be implementable in a CAD package, possibly on a desktop personal computer (PC). The analysis also includes the effects of the discontinuity at the right-angled bends, and the feedback capacitances where the lead-out bridge crosses the spiral turns.

II. General Method of Analysis

The main part of the analysis is based on transmission-line theory, treating the metallized lines of the component as microstrip structures, for which there is a wealth of analysis in the literature [6], [7]. The overwhelming difficulty in this analysis is the problem of multicoupled-line structures, and to derive the parameters of each line section when influenced by all the other lines parallel to it. Methods of analysis of these types of structure do exist [8], [9], but are very difficult to implement in this case as the problem is compounded by the fact that not all the line sections are of the same length, so a particular line section will be parallel with different numbers of other lines at different points along its length. Therefore, a different approach to the problem is required.

The method adopted, which may not perhaps be mathematically rigorous, appears to give sufficiently accurate results to be of some use. In this approach, the multiline problem is broken down into a series of two-parallel-line structures, which are all in parallel with each other, as shown diagrammatically in Fig. 2. Here, the three sub pairs of lines can be considered to be in parallel with each other when we are considering the effect of the multitransmission-line system on the parameters of line section number 1. The two-parallel-line microstrip structure has been widely examined in the past and analyses of varying complexity and accuracy exist. Using this method, each of the line sections of the component can be examined in turn, and each possible two-line structure with which it is associated can be analyzed to derive the transmission-line parameters of the section. If these are expressed in terms of Y-parameters, then when all the possible combinations have been analyzed, the overall Y-parameters of a particular line section is given by the sum of the Y-parameters from each two-line analysis. If this process is repeated for each of the line sections and the Y-matrices converted to chain ($ABCD$) matrices, the product of this series of chain matrices gives the overall chain matrix for the component, which can then be converted into S-parameters as required.

III. Analysis Details

Looking closer at the details of the analysis, a method for analyzing single and coupled microstrip lines to derive such parameters as characteristic impedance and effective dielectric constant is required. The most accurate and easily implemented routine is generally acknowledged to be that of Bryant and Weiss [10], and this routine was adopted for the development stages of this analysis. This routine can be used for both single and two-coupled line structures, requiring as input the width of line, spacing between coupled lines, thickness and relative dielectric constant of the dielectric layer, and the height of an optional upper ground plane. The structure is treated in a rigorous manner using a dielectric Green's function to calculate the line capacitances of the structure with and without the dielectric present. From these parameters, the characteristic impedance, effective

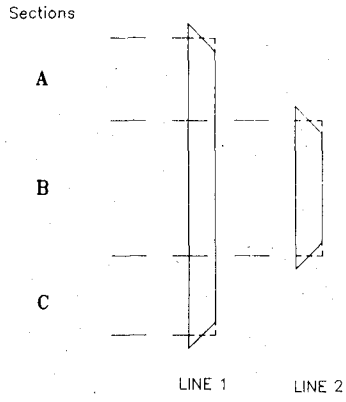

Fig. 3. Typical line pair structure.

dielectric constant, and velocity of propagation are given by

$$\epsilon_{\text{eff}} = C/C_0 \tag{1}$$

$$v = c/\sqrt{\epsilon_{\text{eff}}} \tag{2}$$

$$Z_0 = 1/\left(cC\sqrt{\epsilon_{\text{eff}}}\right) \tag{3}$$

where C is the line capacitance per unit length, C_0 is the line capacitance per unit length without the dielectric, ϵ_{eff} is the effective dielectric constant, v is the velocity of wave propagation, c is the velocity of light in vacuo ($= 2.997925 \times 10^8$ m/s), and Z_0 is the characteristic impedance of the microstrip line. For the case of the coupled lines, these parameters are calculated for both the even and odd modes of propagation.

Consider now in more detail a typical line pair structure which has to be analyzed, as shown in Fig. 3. We wish to derive the Y-parameters of the particular line under consideration (say line 1). First, the ends of the lines are considered to be squared off at the midpoints, as shown by the dotted lines. Now the analysis may have to be broken up into a maximum of three parts, depending on the particular geometry under consideration. In this case, there are three sections—two uncoupled sections either side of a coupled line section, as designated A, B, and C. For the single sections A and C, the single-line parameters are derived using the Bryant and Weiss routine, and the coupled-line odd- and even-mode parameters are also derived from the same routine for the coupled section B. From these parameters, the phase constants of the line sections are given by

$$\beta_A = 2\pi f l_A / v_A \tag{4}$$

$$\beta_C = 2\pi f l_C / v_C \tag{5}$$

$$\beta_B^e = 2\pi f l_B / v_B^e \tag{6}$$

$$\beta_B^0 = 2\pi f l_B / v_B^0 \tag{7}$$

where l_A, l_B, and l_C are the lengths of the sections A, B, and C, f is the frequency, v_A, v_B, and v_C are the propagation velocities of the transmission line sections A, B, and C, and the superscripts e and o refer to the even and odd modes for the coupled-line section.

To derive the overall propagation constant for each line section

$$\gamma = \alpha + j\beta \tag{8}$$

we need to derive the attenuation constant α, which is calculated by considering the losses in the transmission-line structure. These losses consist of two components: dielectric loss and conductor loss. The closed-form equations given by Pucel *et al.* [11] lend themselves very well to this analysis.

Although these equations were derived for a single microstrip line, they can be applied to the odd and even modes of coupled lines, using the appropriate characteristic impedance and electrical length.

So the various propagation constants are now given by

$$\gamma_A = \alpha_A + j\beta_A \tag{9}$$

$$\gamma_B^e = \alpha_B^e + j\beta_B^e \tag{10}$$

$$\gamma_B^0 = \alpha_B^0 + j\beta_B^0 \tag{11}$$

$$\gamma_C = \alpha_C + j\beta_C. \tag{12}$$

In order to derive the overall parameters of the line, it will be necessary to cascade the chain matrices of the three sections, A, B, and C. The chain matrices are derived from the propagation constants and the characteristic impedances of the line sections; thus [6]

$$\begin{vmatrix} A & B \\ C & D \end{vmatrix} = \begin{vmatrix} \cosh(\gamma) & Z_0 \sinh(\gamma) \\ Y_0 \sinh(\gamma) & \cosh(\gamma) \end{vmatrix} \tag{13}$$

where

$$Y_0 = 1/Z_0. \tag{14}$$

In the case of the coupled-line section, the odd- and even-mode parameters are averaged to obtain an effective propagation constant and characteristic impedance prior to the calculation of the chain matrix. The impedance is derived from the geometric average since $Z_0^2 \simeq Z_{oe} Z_{oo}$. The propagation constant is given by the arithmetic average [6].

After cascading the three chain matrices as required, the overall chain matrix is converted to a Y matrix, and the next line-pair structure involving the line section under consideration can be analyzed. Having derived all the Y matrices involving this particular line section, these matrices are all summed to derive the effective Y matrix of the line section, having taken account of all the parallel line sections. This is converted to a chain matrix, and when all such chain matrices have been derived for each line section, the matrices are cascaded in the correct order to derive the overall chain matrix of the component.

In developing the analysis, the discontinuity of the right-angled bend in the microstrip line at the corners was considered. The equivalent circuit given by Garg and Bahl [12] was used. The chain matrix of this equivalent circuit was derived, and included between each line section matrix when the chain matrices are cascaded. The discontinuity of a microstrip bend can be minimized by chamfering of the corner, but the improvement in performance of these particular types of components resulting from this is minimal, and is rarely done in practice.

IV. The Lead-Out Bridge

The lead-out bridge which connects the center of the spiral to the outer circuitry is an integral part of the component, but has often been ignored in other analyses. The bridge may either go above or below the other line sections depending on the particular manufacturing procedure. There are two aspects to the effect of the bridge: the extra line length introduced by the lead out, and the parasitic feedback where the bridge crosses the other line sections.

In the simplest form of analysis, the bridge is treated as an extra length of microstrip transmission line; from its geometry, the corresponding chain matrix is derived in the same way as the other line sections, and the matrix is cascaded onto the end of the other matrices. No coupling between parallel line sections is considered, as the bridge is offset in height from the other lines,

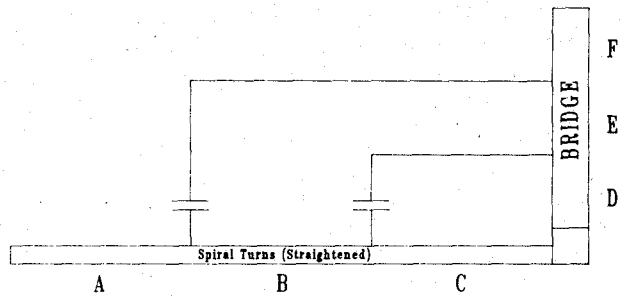

Fig. 4. Equivalent circuit of inductor including feedback capacitances.

so a different routine would have to be implemented to take this into account.

In considering the feedback effects of the bridge, there is considered to be lumped parasitic capacitance between the bridge and a particular line section. The capacitance is further considered to be like a parallel plate component, given by

$$C_f = \epsilon_0 \epsilon_r w \cdot w_B / h_B \tag{15}$$

where w_B is the width of the bridge and h_B is the height of the bridge above or below the line. The capacitance can be considered in this form since $h_B / w_B \ll 1$. ϵ_r in this case is the relative dielectric constant of the material in between ($\epsilon_r = 1.0$ for an airbridge structure). The inclusion of this feedback effect complicates the analysis procedure somewhat. For example, the equivalent circuit of the structure shown in Fig. 1 can be considered as that shown in Fig. 4. Here, the line sections have been straightened out (effectively what happens when the various chain matrices are cascaded). A series of feedback capacitances connect points on the bridge to points on the line sections.

To evaluate the effect of these feedback routes, a flow diagram approach implementing Mason's "nontouching loop" rule was considered. However, the number of possible loops for even a two-turn spiral component becomes immense, and to derive a general formulation for this method becomes virtually impossible. So another matrix method was adopted whereby the Y parameters of various subsections were derived. These subsections are in parallel with the feedback capacitances, the Y matrices of which are easily derivable. In the example of Fig. 4, knowing the chain matrices of each of the sections, including the subdivided bridge, the chain matrix for subsections C and D is converted to a Y matrix, and summed with the parallel Y matrix of the feedback capacitance. This overall Y matrix is converted to a chain matrix. This is cascaded with the chain matrices for sections B and E, converted to a Y matrix, and summed with the capacitor Y matrix. This process is repeated until the complete component has been described. Although this process appears somewhat complex, it is in fact straightforward to implement in a computer algorithm.

V. Implementation of the Analysis

The development of this analysis up to the present time has been performed on an Amdahl 580 computer using FORTRAN 77 programming language. This fast and powerful mainframe handles the described algorithms quickly and efficiently. However, by far the largest CPU time is taken by the Bryant and Weiss routine for calculation of the coupled line parameters, and which is called up as a subroutine to the main algorithm. To implement this analysis on a smaller, less powerful machine, the Bryant and Weiss routine could not be used, as the computation time would be prohibitive. As one of the objects of this work was to derive a package suitable for implementation in a CAD package suitable for a desktop PC, an alternative procedure for calculating the coupled line parameters must be sought. One alternative which was examined was that of Garg and Bahl [13]. These authors have derived semi-empirical design equations for the odd- and even-mode capacitances of a pair of coupled lines, and from these were derived the characteristic impedances, effective dielectric constants, and wave-propagation velocities required in this analysis. With the improvements suggested by Bedair [14] for the odd-mode capacitances, a very simple and fast algorithm can be used in place of the time-consuming Bryant and Weiss routine. Results are presented in the next section comparing the two routines. Comparing the speeds for implementation on the Amdahl, for the test component described below, the CPU times per frequency point were 22 s using Bryant and Weiss, and 0.7 s using Garg and Bahl.

The data requirements of the program are as follows. The program requires that the width of all the lines (but not the bridge) be the same, and currently only a single dielectric substrate can be accommodated (see Section VII). The program requires the linewidth (w), substrate thickness (h), substrate relative dielectric constant (ϵ_r), and loss tangent ($\tan\delta$), metallization thickness (t), and resistivity (ρ_m). For the bridge, the length, thickness, width, height above/below lines, and relative dielectric constant of dielectric between the bridge and the lines is required. concerning the geometry of the lines, the number of line sections, and the x, y coordinates of each of the line ends is required. Finally, the frequency points at which the analysis is performed are also required. The program assumes that the lines are parallel to the $x-y$ axes used to define the coordinates of the lines, and that the bridge is opposite the first line section, i.e., the bridge crosses line-section numbers 3, 7, 11, etc. However, it would only take minor programming changes to eliminate these assumptions—the aim has been simplicity allied with completeness.

VI. Results

A test component of known geometry was obtained. This was a 3 1/2-turn spiral on a gallium arsenide (GaAs) substrate with an airbridge. The dimensions of the component are shown in Fig. 5. Using values of $\epsilon_r = 12.9$, $\tan\delta = 5 \times 10^{-4}$, $t = 5\,\mu$, ρ_m (Au) $= 2.4 \times 10^{-8}\,\Omega$m, the theoretical S_{11} and S_{21} values for the Bryant and Weiss and Garg and Bahl routines are compared in Fig. 6(a) and (b), over a frequency range 1–12 GHz, with a terminating impedance of 50Ω. There is a slight difference between the two results, which becomes larger with frequency, but the massive saving in CPU time justifies the use of the Garg and Bahl routine, and the implementation of such a routine would be vital for use on a smaller machine.

Measurements were made on the test component, which was bonded into an alumina subcarrier and fitted into a microstrip measurement jig. Measurement of S-parameters were performed on an automatic network analyzer, with calibration performed using 3.5-mm coaxial calibration pieces. The S-parameters of the component were de-embedded from the measured parameters using models for the SMA launchers, microstrip lines, and bond wires. The measurements were repeated a number of times in order to derive error bars to the measurements from the experimental repeatability data. A comparison of the theoretical and measured S_{11} and S_{21} results are shown in fig. 7(a) and (b). Reasonably good agreement is obtained, with increasing deviation at higher frequencies.

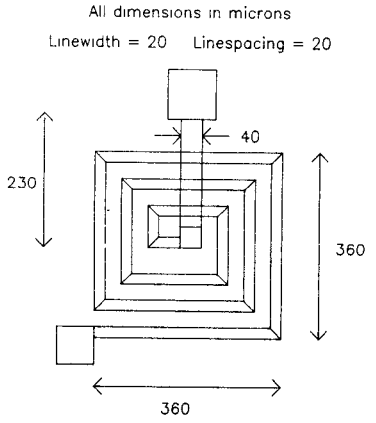

Fig. 5. Dimensions of test inductor.

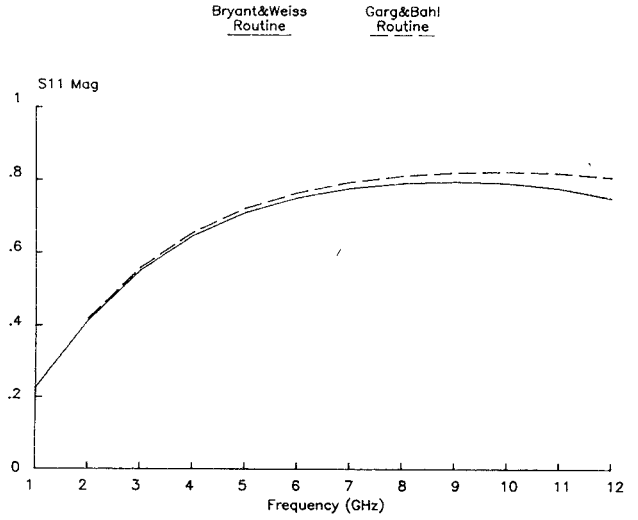

Fig 6(a). Comparison of routines—Theoretical S_{11} of test inductor.

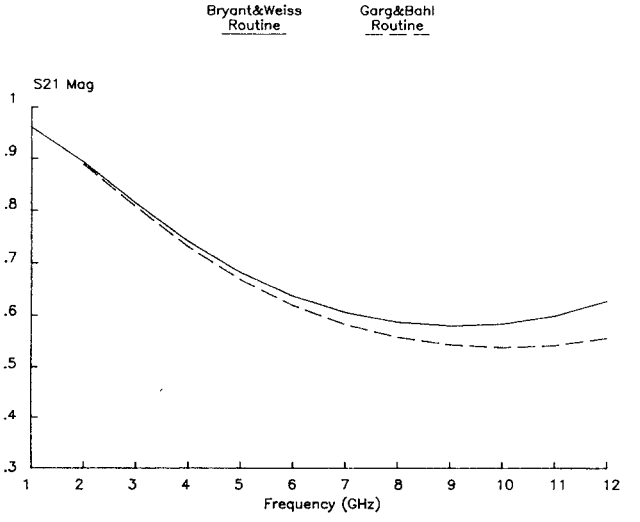

Fig. 6(b). Comparison of routines—Theoretical S_{21} of test inductor.

These theoretical results can be used to derive an equivalent circuit model for the inductor by optimizing the values of the equivalent circuit components to fit the calculated S-parameters. This has been done for the component considered here, and an equivalent inductance of 3.0 nH with a Q of around 60 at 6 GHz was derived.

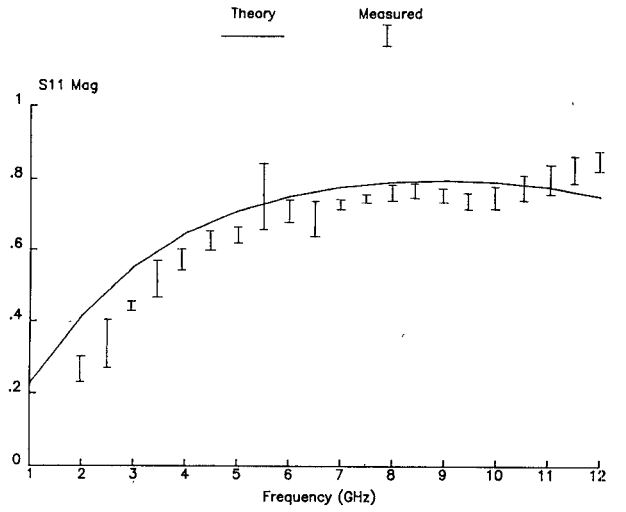

Fig. 7(a). Comparison of theoretical and measured inductor S_{11}.

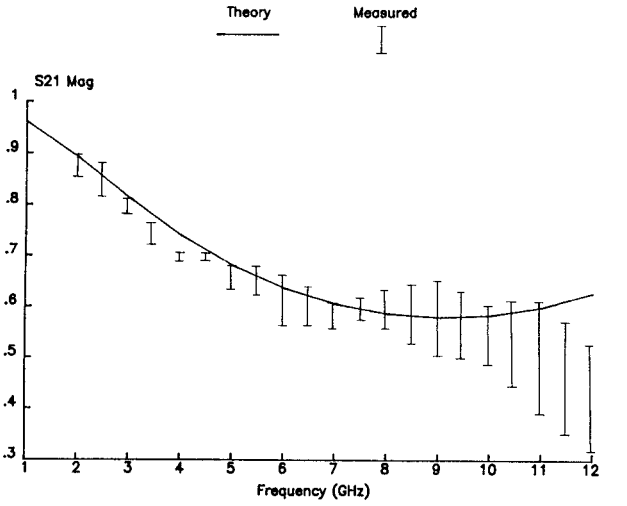

Fig. 7(b). Comparison of theoretical and measured inductor S_{21}.

VII. Conclusions

A novel approach to the solution of multicoupled transmission-line structures has been applied to the analysis of square spiral inductors on dielectric substrates. Good agreement between theoretical and measured results has been demonstrated over the frequency range within which these components are generally used. Routines with both higher accuracy/higher CPU time and lower accuracy/lower CPU time have been implemented. The latter is suitable for inclusion in CAD packages, where it may prove a more accurate analysis than currently available routines. For example, the analysis of the test structure is compared with the results from the SuperCompact PC package for the same structure, along with the measured results, in Fig. 8(a) and (b).

Currently, the analysis can only handle a single dielectric layer, which is perhaps unrepresentative of current manufacturing technologies. For example, in GaAs MMIC's, there is often a thin layer of polyimide dielectric on top of the substrate (used as an ion-beam milling stop). However, calculations using a finite-element routine [15], which can be applied to multidielectric structures, has shown in error in line parameters of around 2 percent with the inclusion of this layer compared to the single dielectric layer results. This can be almost entirely offset by using a

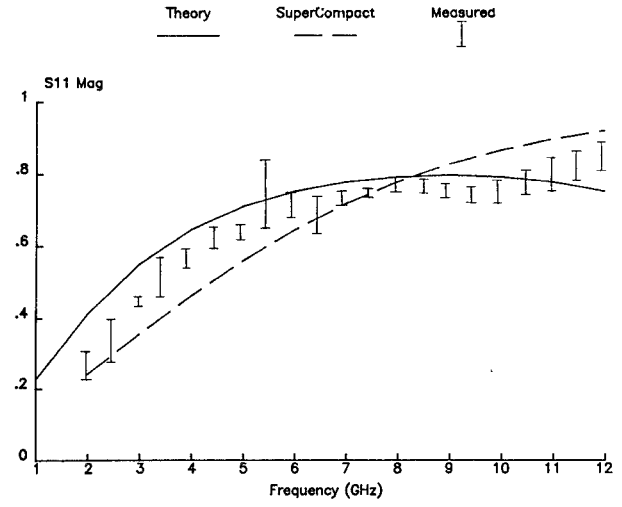

Fig. 8(a). Comparison of method with SuperCompact PC and measured S_{11}.

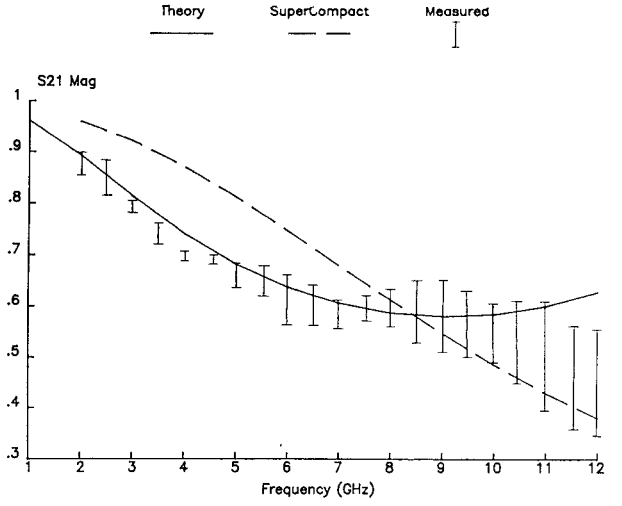

Fig. 8(b). Comparison of method with SuperCompact PC and measured S_{21}.

decreased value for the substrate thickness. For example, it has been found that a 195-μm substrate of pure GaAs has almost the same characteristics as a 200-μm substrate with a 2-μm polyimide layer on top, for the same linewidth. However, it would be preferable to be able to include a suitable routine which could calculate single and coupled line parameters for multidielectric structures.

Acknowledgment

Thanks go to Plessey Research (Caswell) Ltd., Towcester, U.K., for supplying the test inductor and measurement jig design.

References

[1] H. M. Greenhouse, "Design of planar rectangular microelectronic inductors," *IEEE Trans.*, vol. PHP-10, no. 2, pp. 101–109, June 1974.

[2] D. Cahana, "A new transmission line approach for designing spiral microstrip inductors for microwave-integrated circuits," in *MTT-S Int. Microwave Symp. Dig.* (Boston, MA), pp. 245–247.

[3] I. Wolff and G. Kibuuka, "Computer models for MMIC capacitors and inductors," in *Proc. 14th Euro. Microwave Conf.* (Liege, Belgium), Sept. 10–13, 1984, pp. 853–858.

[4] M. Parisot, Y. Archambault, D. Pavlidis, and J. Magarshack, "Highly accurate design of spiral inductors for MMIC's with small-size and high-cut-off frequency characteristics," in *MTT-S Int. Microwave Symp. Dig.* (San Francisco, CA), 1985, pp. 106–110.

[5] A. J. Baden-Fuller and A. M. Parker, "Equivalent circuit of microstrip spiral inductor—Circuit generation by computer," *Electron. Lett.*, vol. 21, no. 7, pp. 279–280, Mar. 28, 1985.

[6] T. C. Edwards, *Foundations of Microstrip Circuit Design*. New York: Wiley, 1981.

[7] K. C. Gupta, R. Garg, and I. J. Bahl, *Microstriplines and Slotlines*. Dedham, MA: Artech House, 1979.

[8] E. Yamashita and K. Atsuki, "Analysis of microstrip-like transmission lines by nonuniform discretization of integral equations," *IEEE Trans. Microwave Theory Tech.*, vol. MTT-24, pp. 195–200, Apr. 1976.

[9] J. B. Davies and D. Mirshekar-Syahkal, "Spectral domain solution of arbitrary coplanar transmission line with multilayer substrate," *IEEE Trans. Microwave Theory Tech.*, vol. MTT-25, pp. 143–146, Feb. 1977.

[10] T. G. Bryant and J. A. Weiss, "Parameters of microstrip transmission lines and of coupled pairs of microstrip lines," *IEEE Trans. Microwave Theory Tech.*, vol. MTT-16, pp. 1021–1027, Dec. 1968.

[11] R. A. Pucel, D. J. Masse, and C. P. Hartwig, "Losses in microstrip," *IEEE Trans. Microwave Theory Tech.*, vol. MTT-16, pp. 342–350, June 1968 (Also see, "Corrections," *IEEE Trans. Microwave Theory Tech.*, vol. MTT-16, no. 12, p. 1064, Dec. 1968).

[12] R. Garg and I. J. Bahl, "Microstrip discontinuities," *Int. J. Electron.*, vol. 45, no. 1, pp. 81–87, 1978.

[13] R. Garg and I. J. Bahl, "Characteristics of coupled-microstrip lines," *IEEE Trans. Microwave Theory Tech.*, vol. MTT-27, pp. 700–705, July 1979.

[14] S. S. Bedair, "On the odd-mode capacitance of the coupled microstrip-lines," *IEEE Trans. Microwave Theory Tech.*, vol. MTT-28, pp. 1225–1227, Nov. 1980.

[15] P. R. Shepherd and P. Daly, "Modeling and measurement of microstrip transmission line structures," in *MTT-S Int. Microwave Symp. Dig.* (St. Louis, MO), 1985, pp. 679–682. Also published in the Symposium Issue of *IEEE Trans. Microwave Theory Tech.*, vol. MTT-33, pp. 1501–1506, Dec. 1985.

Characteristic Impedance of Transmission Lines with Arbitrary Dielectrics under the TEM Approximation

YANG NAIHENG AND ROGER F. HARRINGTON, FELLOW, IEEE

Abstract — **This paper gives a procedure for computing the characteristic impedances of TEM or quasi-TEM transmission lines with arbitrary cross sections and arbitrary dielectrics. Special consideration is given to conductors of finite cross-sectional extent. The solution is obtained by the method of moments using pulse functions for the expansion of charge density and point matching for testing. Numerical examples are given and compared with solutions obtained by other methods.**

I. Introduction

Recently, a general procedure for computing the transmission-line parameters for a multiconductor transmission line in a multilayered dielectric medium was published [1]. The solution was obtained by the method of moments [2] using pulse functions for expansion of the free and bound charge densities, and point matching for testing. The solution made use of the fact that the ground conductor was an infinite conducting plane. If no infinite conducting plane is present, the solution must be modified.

This paper considers the modification for a two-conductor transmission line of arbitrary cross section with arbitrary numbers of dielectrics. Strictly speaking, if the field exists in two or more different dielectrics. the transverse electromagnetic (TEM)

Manuscript received September 12, 1985; revised November 5, 1985. This work was supported in part by Dupont Connector Systems, Camp Hill, PA 17011.

Y. Naiheng is with the Nanjing Research Institute of Electronic Technology, Nanjing, People's Republic of China.

R. F. Harrington is with the Department of Electrical and Computer Engineering, Syracuse University, Syracuse, NY 13210.

IEEE Log Number 8407188.